sures for each of the gases. Also, high supersaturations without cavitation were not dependent on confinement of the water in capillaries of small dimensions, such as is necessary for avoiding cavitation in water under tensile stress (4); there was little change in the cavitation properties when capillaries of dimensions ranging from 0.15 to 2.5 mm in inner diameter were used.

Since experimental reproducibility was excellent with different samples of glass, water, and gas, and since the pressure range from the condition of no cavitation to the beginning of massive cavitation was small and rather well defined for each of the gases, the pressures for beginning massive cavitation (Table 1, column 4) may represent the approximate value for *de novo* bubble formation at the water-gas interface and, possibly, also in the water body. The highest supersaturations without any cavitation (Table 1, column 3) represent the lowest possible limits for such bubble formation. The highest such value that had been obtained previously was 70 atm for nitrogen (5).

Since the pressure for bubble formation increases with decreasing gas solubility, the gas concentration rather than the pressure (that is, tension) appears to be the determining factor. In view of this, Haldane's classical maximum supersaturation limit for

avoiding the "bends" (6) should be examined and possibly modified for gases other than nitrogen.

E. A. HEMMINGSEN
*Physiological Research Laboratory,
Scripps Institution of Oceanography,
University of California at San Diego,
La Jolla 92037*

References and Notes

1. R. B. Dean, *J. Appl. Phys.* **15**, 446 (1944); E. N. Harvey, D. K. Barnes, W. D. McElroy, A. H. Whiteley, D. C. Pease, K. W. Cooper, *J. Cell. Comp. Physiol.* **24**, 1 (1944).
2. Recent reviews of this field can be found in *The Physiology and Medicine of Diving and Compressed Air Work*, P. B. Bennett and D. H. Elliot, Eds. (Baillière Tindall & Cassell, London, 1969), and in *Underwater Physiology*, C. J. Lambertsen, Ed. (Williams & Wilkins, Baltimore, 1967).
3. This was the highest value obtained before breakage of the capillary tubes. Because explosive breakage sometimes occurred at lower pressures as well, care must be taken during the experiments.
4. L. J. Briggs, *J. Appl. Phys.* **21**, 721 (1950).
5. F. B. Kenrick, K. L. Wismer, K. S. Wyatt, *J. Phys. Chem.* **28**, 1308 (1924).
6. With nitrogen as the main gas, in vivo bubbles are avoided by maintaining a ratio of supersaturation tension to external pressure of approximately 2 : 1, or less [J. S. Haldane and J. G. Priestley, *Respiration* (Yale Univ. Press, New Haven, 1935), pp. 327–362]. Most decompression procedures have made use of this ratio (see references in 2).
7. E. Douglas, *J. Phys. Chem.* **68**, 169 (1964); R. F. Weiss, personal communication.
8. Supported by grant GM 10521 from the Department of Health, Education, and Welfare.

13 November 1969; revised 12 January 1970 ∎

Uranium Localization on Hydroxyapatite by Analysis of Fission Fragment Tracks

Abstract. *The distribution of enriched uranium on individual hydroxyapatite crystals after an exchange reaction has been investigated by means of thermal neutron irradiation followed by electron microscopic analysis of fission fragment tracks in plastic support films. One uranyl ion for every two to three surface calcium ions became associated with the mineral but in a nonuniform distribution that strongly favors crystal end regions.*

Induced fission of uranium-235 in thin films has been shown to produce damage tracks in the films along the path of the ejected high-energy fission fragments (1–3). This physical process was first proposed as the basis of a high-resolution biological tracer system by Malmon (4), who also experimentally demonstrated the feasibility of the technique. In this report I describe the application of this new tracer technique to uranyl ion–hydroxyapatite exchange experiments. Because the experimental results could not have been obtained with other high-resolution tracer methods presently in use, a detailed comparison is included between the characteristics of the new system and other tracer techniques.

All high-resolution biological tracer systems in use at present are based upon (i) specific histochemical precipitation reactions, or (ii) immunochemical reactions that use an electron-dense tag on one component, or (iii) electron microscopic radioautography. All these basic processes are subject to numerous influences that can produce positive or negative artifacts, alter response threshold and sensitivity capabilities, and lead to nonuniform results from one area to another in a single sample (5). Also dissolution or

loss of a precipitate (6) or latent image (7) can occur, diffusion can cause movement of established markers from their original position (8), and accurate quantitation of final results is difficult or impossible.

Maximum resolution capabilities of histochemical and immunochemical methods are limited by the minimum size of the precipitate or the electron-dense tag formed to areas of the order of 30 to 150 Å in diameter; resolution limits of electron microscopic radioautography are probability circles of 1000 to 3000 Å diameter or more (9).

Most of the deficiencies mentioned which are inherent in the above techniques cannot occur in the new system. The cumulative dose of thermal neutrons given the samples completely determines the fraction of uranium atoms that will undergo fission wherever they are located (10). Essentially all the fission events produce damages to thin plastic films with a relatively constant proportion of these having the configuration of tracks (2, 4). Accordingly, the sensitivity of the system is uniform in all areas of a sample and dose-controllable, and reasonably good quantitative estimations of the uranium content can be made from the numbers of tracks observed
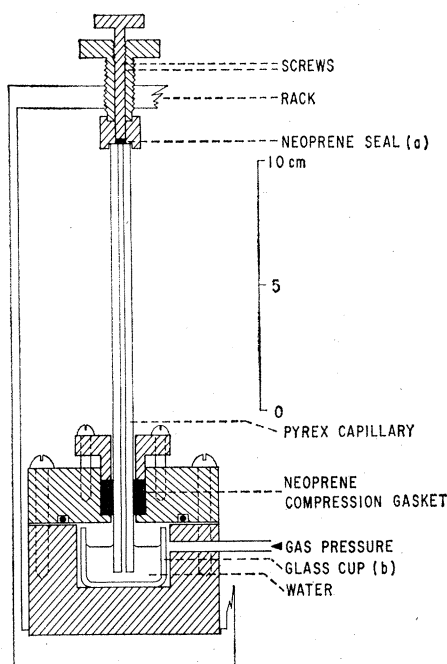

Fig. 1. Apparatus used for the experiments. Hatched areas signify parts made of brass.

Labels in figure: SCREWS, RACK, NEOPRENE SEAL (a), 10 cm, 5, 0, PYREX CAPILLARY, NEOPRENE COMPRESSION GASKET, GAS PRESSURE, GLASS CUP (b), WATER

in an area of interest. The tracks are readily distinguished from normally appearing biological structures and staining artifacts (4), and, once it has formed in the thin film at the time of fission, a damage track cannot vanish or migrate from its original position. Negative artifacts are therefore not possible, and positive artifacts can only result from contamination of a sample by some other fissionable isotope or conceivably by the intersection of certain highly ionizing particles with the film, both of which should be extremely rare events in practice (11).

Resolution limits obtainable on the basis of the fission fragment tracks or fissionographic system are approximately 10 to 50 Å in a direction normal to the axis of a track; in the axial direction resolution limits can range from 100 to 200 Å up to the full length of the track, depending upon the particular experimental conditions (3, 4). The experiments described below depend upon resolution in the normal direction only.

Synthetic crystals of hydroxyapatite (HA) were prepared by a modification (12) of a method of Hayek and Newesely (13). Ammonium phosphate dissolved in an ammonium hydroxide solution (pH 12) was added slowly to a solution of calcium nitrate dissolved in an ammonium hydroxide solution (pH 12) at 25°C in an environment free of carbon dioxide. To promote crystal maturation the suspension was then boiled for 100 hours during which time the pH was continuously maintained at 10.0 by passing ammonia through the solution. The product after washing was stored wet for several months prior to use. The combined results of analyses by x-ray diffraction, electron microscopy, and infrared spectroscopy indicated that the material was a well-crystallized, essentially carbonate-free hydroxyapatite with a mean crystal length of 700 Å.

Exchange reactions were carried out at room temperature with suspensions having a mass-to-volume ratio of 0.125 g/liter and an initial uranyl ion concentration (as the acetate) of 1.0 mM. The pH was adjusted, when necessary, by the addition of acetic acid or ammonium hydroxide. The concentration of uranyl ion left in solution at different times was measured by liquid scintillation counting of samples aspirated through a Millipore filter to remove the solid phase. In preliminary

studies to determine whether coprecipitation might occur, I used only the solution phase of the HA suspension; the results demonstrated that precipitates can form at low or at high pH. X-ray diffraction studies of these materials characterized the product obtained at pH 3.0 as calcium uranyl phosphate hydrate (meta-autunite) and the material formed at pH 10.0 as a distinctly different compound, probably a uranium oxide. Conditions of low pH were selected for the reaction to avoid net accretion of mineral during the process, and at the pH used complete dissolution of the HA crystals could be demonstrated after long times. Preliminary studies of this exchange reaction at pH 3.0 over a period of 11 days showed maximum uranyl ion loss from solution in the first 10 minutes; the final crystalline product at 11 days, as determined by x-ray diffraction studies, was entirely meta-autunite with no evidence of hydroxyapatite. The product collected at 15 minutes, however, did show persistence of the HA diffraction pattern and no evidence of a second crystalline phase. Serial counts of the solvent phase made with ^{45}Ca-labeled HA in acetic acid solution (pH 3.0) showed no change over 15 minutes, an indication that no significant crystal dissolution occurred. Electron microscopic studies of this material also failed to demonstrate sig-
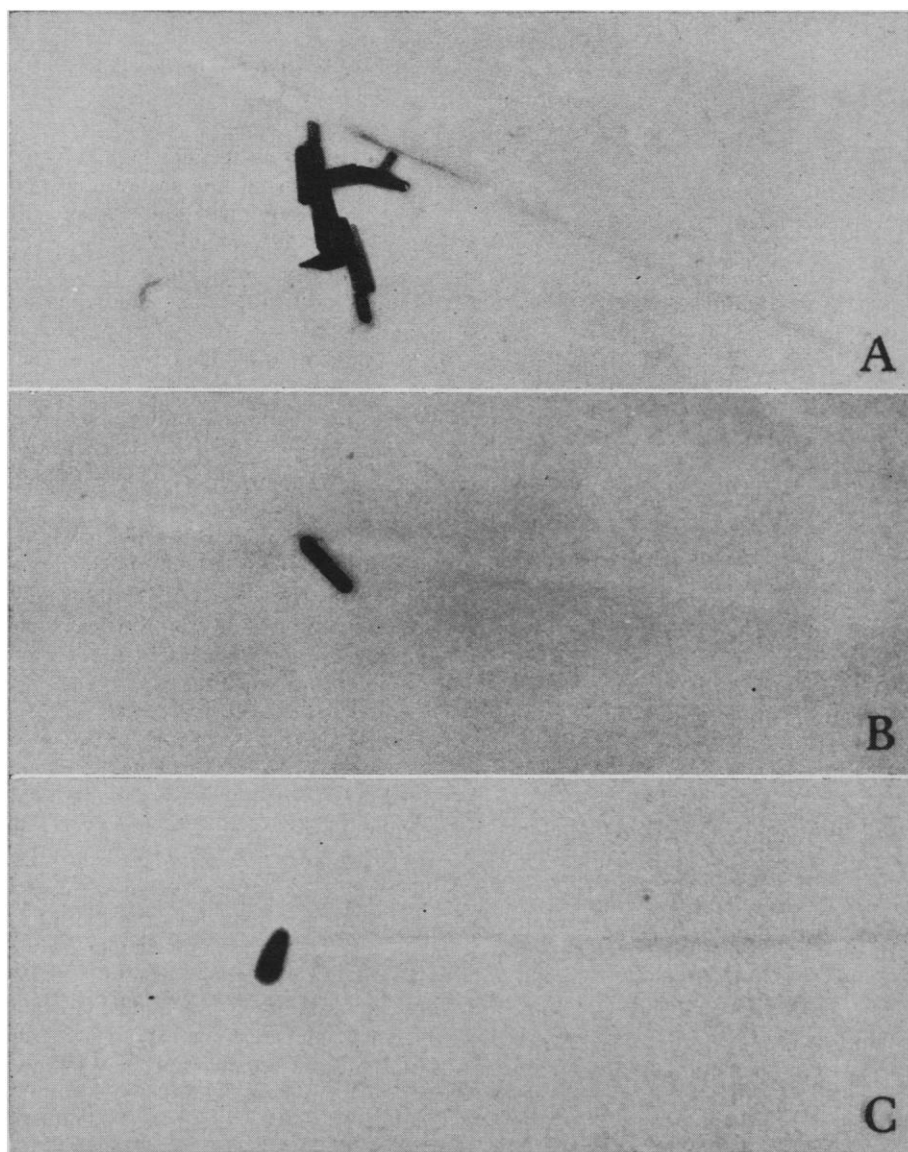

Fig. 1. Electron micrographs of uranium fission fragment tracks intersecting crystals of synthetic hydroxyapatite. (A and B) Representative tracks apparently related to the extreme ends of the respective crystals (× 69,000 and × 80,000, respectively). (C) Track intersecting the middle regions of a crystal (× 72,000). All preparations were lightly coated with chromium (calculated thickness, 6 Å) before irradiation.

Table 1. Uranium and hydroxyapatite distributions in the reaction after various steps in the procedure.

Stage	UO_2^{2+} (μmole)	HA (μmole)	Tracks (%)
Initial suspension			
Solvent phase	5.0	0	
Solid phase	0	0.625	
After 15 minutes reaction			
Solvent phase	3.4		
Solid phase	1.6	0.60	
Removed from solid in washings	1.3		
Final collodion suspension			
Collodion phase	0.06 (20 %)		25
Mineral phase	0.24 (80 %)	0.60	
Crystal end regions			70
Crystal central regions			5

nificant amorphous material or a second distinctive crystal form, and this product collected after 15 minutes of reaction time was used in the subsequent studies.

The partitioning of the enriched uranium (14) between the solid and solvent phases in the reaction is indicated in Table 1. The relatively large amount of uranyl ion lost in washings may represent the part loosely associated with the crystals in hydration shell water. Similar large amounts of calcium and phosphate have been shown to be displaced in dilution experiments on synthetic hydroxyapatite (15). The uranium remaining in the final solid phase after washing corresponds in amount to approximately one uranyl ion for every three calcium ions located at the surface of the original crystals. This quantitative relationship is consistent with studies of the uptake of uranium by bone ash in which Neuman et al. suggested that a surface ionic exchange process occurred with a ratio of one uranyl ion to every two calcium ions (16).

To investigate the surface distribution pattern of uranium, the crystals after washing in water, acetone, and amyl acetate were suspended in 20 percent collodion. Thin films prepared from this solution were mounted on electron microscope grids, coated with a thin layer of carbon or chromium, and irradiated to a cumulative thermal neutron flux of 10^{16} neutron/cm². Observation of the irradiated sample by electron microscopy confirmed that an adequate number of fission fragment tracks were formed, and the majority of tracks seen intersected visible crystals (Fig. 1). The observation that about 25 percent of the tracks did not intersect crystals at any point is in agreement with the results of analysis of the uranium distribution between the collodion and the mineral (Table

1). Dispersion of crystals was incomplete, even in fairly dilute preparations, but a sufficient number of isolated crystals were observed to permit the study of individual crystal-track intersections.

Solitary crystals in electron micrographs were divided transversely into four segments of equal length, and tracks were designated as end or central (quarters) according to the segment of a crystal intersected. Tracks intersecting more than one crystal and tracks partly intersecting both an end and a central segment were discarded. Uranium uniformly distributed on the crystal surfaces should lead to approximately equal numbers of tracks in the two categories because the amount of surface area is approximately the same in each segment. However, the majority of the tracks observed were in the end regions and frequently appeared to be closely related to the extreme ends of the crystals (Fig. 1). Statistical analysis of the track data indicated that the hypothesis of a uniform surface exchange pattern for uranyl ion under the conditions of these experiments is probably not valid ($P = .02$). More extensive data and statistical work is required to critically evaluate the nonuniformity in detail.

Although differences in the chemical properties and reactivity between the sides and ends of hydroxyapatite crystals might be anticipated from the prevalent crystal shape and detailed considerations of atomic structure (17), there appears to be no published data on small crystals directly related to this point for comparison that do not involve crystal accretion. Even in the simplified system used (a relatively pure hydroxyapatite and a limited number of ionic species), it is impossible to define exact surface chemical reactions involved. A surface 1 : 2 exchange reactions of UO_2^{2+} for Ca^{2+}

cannot alone account for the observed uranium distribution. The effect on surface reactions of crystal imperfections, especially screw dislocations, is undoubtedly great but cannot be separately evaluated in these studies (18). The possibility of a limited amount of complex formation or of more involved reactions than simple surface exchange of uranyl ions for calcium ions cannot be excluded by the infrared spectroscopy and x-ray diffraction analyses. It is likewise difficult to evaluate the possibility of relocation of uranium on the crystals during the washing steps and in the final collodion suspension.

It is possible in principle to extend the fissionographic technique described to the study of any elongated structures capable of taking up fissionable molecules. The growth of large crystals and the effects of poisons and dislocations on surface reactivity could be investigated by use of this technique. Tracks have been identified in thin sections of renal tissue (4), and the study of mineral interfaces in biological hard tissues is one possible application of immediate interest. Critical experimental requirements for any studies are minimum translocation and acceptable losses of sample and label during preparation (increasingly important with samples of high surface area), satisfactory sample dispersion and mounting, an appropriate statistical hypothesis, and the production of adequate numbers of tracks to permit valid statistical conclusions.

ROBERT C. THOMPSON*
National Institute of Dental Research,
National Institutes of Health,
Bethesda, Maryland 20014

References and Notes

1. T. K. Bierlein and B. Mastel, J. Appl. Phys. 31, 2315 (1960); T. S. Noggle and J. O. Stiegler, ibid. 33, 1726 (1962); A. N. Goland, in Studies in Radiation Effects: Series A–Physical and Chemical, G. J. Dienes, Ed. (Gordon & Breach, New York, 1966), vol. 1, p. 159.
2. J. J. Kelsch, O. F. Kammerer, A. N. Goland, P. A. Buhl, J. Appl. Phys. 33, 1475 (1962).
3. A. G. Malmon, ibid. 34, 3634 (1963).
4. ———, Biophys. J. 4, 1 (1964).
5. G. B. Pierce, Jr., J. S. Ram, A. R. Midgely, Jr., Int. Rev. Exp. Pathol. 3, 1 (1964); R. A. Rifkind, K. C. Hsu, C. Morgan, J. Histochem. Cytochem. 12, 131 (1964); P. K. Nakane and G. B. Pierce, Jr., J. Cell Biol. 33, 307 (1967).
6. H. O. Kalimo, H. J. Helminen, A. U. Arstila, V. K. Hopsu-Havu, Histochemie 14, 123 (1968).
7. L. Caro, Progr. Biophys. Mol. Biol. 16, 171 (1966).
8. S. Goldfischer, E. Essner, A. B. Novikoff, J. Histochem. Cytochem. 12, 72 (1964).
9. For example, using emulsion with a mean grain diameter of 1100 Å, L. G. Caro and M. Schnös [Science 149, 60 (1965)] found resolution limits of 1000 Å and 3000 Å for tritium and phosphorus-32, respectively. The

1496

definition of resolution used, the distance at which the developed grain count dropped to 50 percent of maximum, represents far less than 95 percent probability.

10. The fraction of uranium atoms undergoing fission is equal to the product of the reaction cross section and the integrated neutron flux.

11. R. L. Fleischer, P. B. Price, R. M. Walker, R. C. Filz, K. Fukui, M. W. Friedlander, E. Holeman, R. S. Rajan, A. S. Tamhane, *Science* 155, 187 (1967). The possibility of track production by other induced nuclear reactions, such as $^{17}O(n,\alpha)^{14}C$, would not interfere in the present studies on the basis of the estimations of A. G. Malmon [*J. Theor. Biol.* 9, 77 (1965)].

12. B. O. Fowler, personal communication.

13. E. Hayek and H. Newesely, *Inorg. Syn.* 7, 63 (1963).

14. Material used was 93.161 percent enriched uranium-235 as uranyl acetate in acetic acid solution.

15. Y. Avnimelech, *Israel J. Chem.* 6, 375 (1968).

16. W. F. Neuman, M. W. Neuman, E. R. Main, B. J. Mulryan, *J. Biol. Chem.* 179, 325 (1949); *ibid.*, p. 335; *ibid.*, p. 341.

17. D. R. Taves, *Nature* 200, 1312 (1963).

18. J. Arends, B. S. H. Royce, R. Smoluchowski, D. O. Welsh, paper presented at the International Symposium on the Structural Properties of Hydroxyapatite and Related Compounds, Gaithersburg, Maryland, 12–14 September 1968.

19. I thank D. A. Nylen, A. G. Malmon, and B. O. Fowler for valuable help and encouragement in these studies. Supported in part by NIH training grant No. 5 T01-Am-05317-08 and the Bowles Fund of the Children's Hospital of Baltimore. Neutron irradiation obtained through the cooperation of the Armed Forces Radiobiology Research Institute, Bethesda, Maryland.

* Present address: Orthopaedic Research Laboratories, Johns Hopkins Hospital, 601 North Broadway, Baltimore, Maryland 21205.

14 November 1969

Fluid Transport: Concentration of the Intercellular Compartment

Abstract. *Intercellular spaces of* Periplaneta *rectal pads are visible at a magnification of × 100 and distend during fluid uptake. Samples (0.025 to 0.1 nanoliter) obtained by micropuncture from the spaces were consistently more concentrated than the fluid in the rectal lumen. This observation supports the hypothesis of "local" osmosis in epithelial fluid transport.*

Water "transport" across epithelia is a passive consequence of active transport of solutes (1). Thus a basic problem is to explain how solute movement generates a flow of water. One suggestion is that the long, narrow intercellular spaces, which are characteristic of absorptive epithelia, have a functional role in transport by acting as the sites of osmotic gradients (2). According to this hypothesis, solutes are pumped into the spaces, making them hyperosmotic to the cell and lumen, creating the osmotic gradients that bring about water absorption. This concept, which has been termed "local" osmosis (3) may have general application for epithelia such as gall bladder, intestine, and kidney, which have intercellular spaces that are closed off from the lumen but open in the direction of fluid transport (2, 4). However, there has been no demonstration of an osmotic gradient between the intercellular spaces and the lumen, from which the fluid is absorbed. Indirect evidence has come from study of rabbit gall bladder, in which measurements of diffusion potential led to the calculation that the NaCl concentration in the intercellular spaces is about 10 mM higher than in the bathing medium (5). More direct evidence can only be obtained by methods that allow precise determination of the concentration of intercellular fluids. Insect rectal pads offer good opportunities for a direct approach be-cause they have intercellular spaces that are large enough to see with a dissecting microscope, and fluid samples can be collected from them by means of micropuncture. Samples collected from the spaces were consistently hyperosmotic to the rectal lumen during fluid uptake.

Insect rectal pads and papillae are thickenings of the rectal epithelium, composed of tall columnar cells. They function to absorb water and solutes from the fecal material prior to excretion (6). In dehydrated animals absorption of water occurs against an increasing osmotic gradient, and very concentrated fecal material is excreted (6, 7). Rectal pads and papillae have complex systems of intercellular spaces that drain in the direction of fluid uptake, that is, into the hemocoel of the insect (8, 9), and it has been suggested (7, 9, 10) that the spaces are the sites of local osmotic gradients.

Adult male *Periplaneta americana* L. were dehydrated for 4 to 7 days and then anesthetized with CO_2. The rectum was exposed by dissection, cannulated through the anus, and covered with paraffin oil. The cannula was attached to a syringe containing either a fluid resembling colon fluid (11) or a more concentrated fluid (12). The rectal contents were forced into the colon by injecting fluid into the rectum. The junction between colon and rectum was then ligated. The artificial colon fluid was injected in order to simulate the most active absorptive condition in vivo. This occurs after a dry fecal pellet is excreted and dilute colon fluid moves into the rectal lumen. A non-permeant dye (Nigrosine, 1 mg/ml) was added to the injected fluid to provide a dark background, facilitating observations of the intercellular spaces. The prepara-
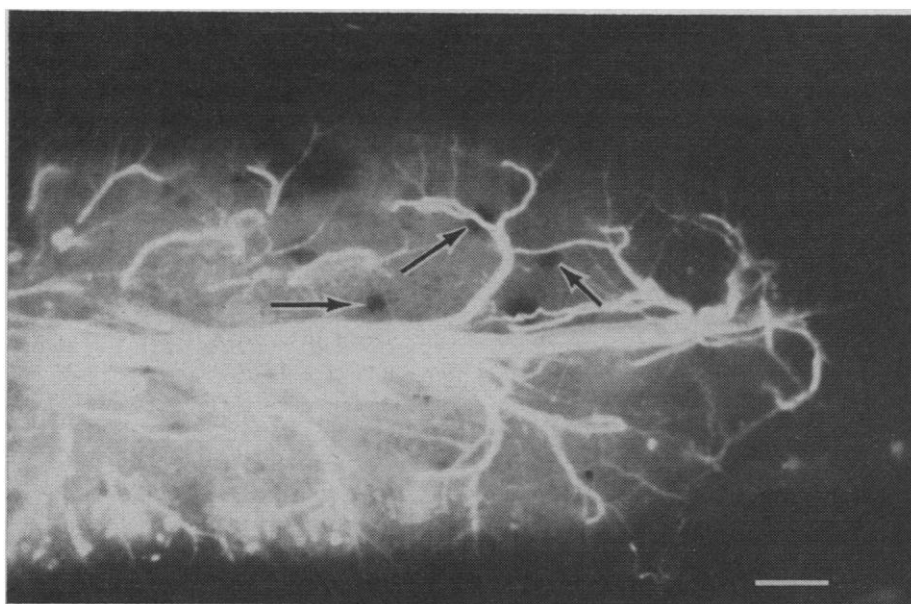

Fig. 1. A portion of a rectal pad as it appears in the dissecting microscope. In this preparation intercellular spaces (arrows) distended within 2 minutes after artificial colon fluid was injected into the lumen. The dark appearance of the spaces is due to the presence of Nigrosine dye in the injected fluid. The rectal pads are richly supplied with tracheae that appear as highly branched tubes. Marker is 0.1 mm.